Article

Valorization of Hazelnut Shells as Growing Substrate for Edible and Medicinal Mushrooms

Federico Puliga *,† , Pamela Leonardi † , Francesco Minutella, Alessandra Zambonelli and Ornella Francioso

Department of Agricultural and Food Sciences, University of Bologna, Viale G. Fanin 40-50, 40127 Bologna, Italy; pamela.leonardi@unibo.it (P.L.); francesco.minutella@studio.unibo.it (F.M.); alessandr.zambonelli@unibo.it (A.Z.); ornella.francioso@unibo.it (O.F.)
* Correspondence: federico.puliga2@unibo.it
† These authors contributed equally to this work.

Abstract: Recently, the cultivation of hazel is undergoing a large expansion. Italy is the world's second largest producer of hazelnuts, with a production of around 98,530 tons in 2019. The processing of hazelnuts produces large amounts of waste, especially woody pericarps, due to the cracking process, generally used for domestic heating, causing air pollution. The high lignin content present in the pericarps makes them a suitable substrate for the cultivation of edible and medicinal mushrooms. To this aim, *Ganoderma lucidum, Lentinula edodes,* and *Pleurotus cornucopiae* were grown and cultivated on different hazelnut-shell-based substrates: Hazelnut Shell (HS), Hazelnut Shell and Wheat Straw (HS-WS), and Wheat Straw mixed with Beech Chips (WS-BC) as control. In vitro mycelial grow rate, the degradation capacity of the lignocellulosic fraction, the biological efficiency, and the qualitative differences between mushrooms growing on different substrates by using Attenuated Total Reflectance–Fourier transform infrared (ATR-FTIR) spectroscopy were investigated. Our results suggested the ability of *G. lucidum, L. edodes,* and *P. cornucopiae* to grow and decay the lignocellulosic fraction of HS. Cultivation trials showed a similar biological efficiency but a different Fruiting Body Production (FBP) in the presence of HS with respect to the control. ATR-FTIR analysis provided a chemical insight for the examined fruiting bodies, and differences were found among the substrates studied. These results provide attractive perspectives both for more sustainable management and for the improvement of mushroom cultivation efficiency.

Keywords: sustainability; mushroom cultivation; wood fungi; ATR-FTIR

1. Introduction

The hazel, *Corylus avellana* L., is the world's leading nut crop with a production of 1,125,178 tons in 2019 [1]. Turkey, Italy, and Azerbaijan are the three lay producers with a production of 776,046; 98,530 and 53,793 tonnes, respectively [1]. Ninety percent of the hazelnuts produced are intended for processing [2], deprived of the woody pericarp, and used in chocolate, pastry, confectionery, as well as in the preparation of numerous foods and liqueurs [3,4].

One of the main concerns associated with hazelnut production is due the large amount of by-products. Hazelnuts are mechanically collected by compact harvesters in-shell covered by husks that are mechanically separated during harvesting. In-shell nuts need to be opened in order to be introduced into the industrial food chain. The woody biomass produced as a result of the cracking process accounts for more than 50% of the total nut weight [5]. Lignin, present in a percentage between 40% and 50%, is the main constituent of the hazelnut shells, followed by hemicellulose and cellulose present in percentages between 13–32 and 16–27 percent, respectively [5–7].

In recent years, there has been marked attention to climate change, the preservation of species biodiversity, environmental sustainability by sustainable and environmentally

friendly use, and the recycling of waste in line with the circular economy approach. Consequently, the scientific community is encouraged to seek new methods and strategies for exploiting the by-products of agricultural activities.

Traditionally, hazelnut shells (HS) are mainly used as a boiler fuel for domestic heating causing air pollution [8–10] and for landscaping [11]. Several studies have been conducted in order to enhance and valorize this waste by-product with the aim to obtain new materials, chemical compounds, and bioactive ingredients. In particular, HS were found to be suitable for the production of particleboard and Medium Density Fiberboard (MDF) [12,13], activated carbons capable of adsorbing and removing different heavy metals and CO_2 [14–22], antioxidant phenolics [6,23–26], fermentable sugars and xylooligosaccharides [11,27], hydrogen production [28,29], ethanol [30] and some prebiotic compounds [31].

Mushrooms are considered an important source of food and biologically active compounds with several medicinal proprieties [32]. Various lignocellulolytic mushrooms such as oyster mushrooms, shiitake, and *Ganoderma* sp. are cultivated on different pasteurized or sterilized lignocellulosic substrates. While oyster mushroom (*Pleurotus* spp.) and shiitake (*Lentinula edodes* (Berk.) Pegler) are cultivated worldwide for their culinary qualities [33,34], *Ganoderma lucidum* sensu latu is the most important medicinal mushroom, and it is specifically cultivated for its pharmacological activities [35]. Moreover, mushrooms can be cultivated on several agricultural wastes, which can be sustainably recycled in the principles of circular economy [36].

Some previous works report the possibility of using the hazelnut husk and hazelnut leaves as basal ingredients for substrate preparation in *L. edodes* and *Pleurotus* cultivation [10,37,38], but no reference was found by the authors regarding the use of HS as substrate for mushroom cultivation. Due to the high lignin content, this by-product can be used as a substrate for the cultivation of lignocellulolytic mushrooms.

Fourier transform infrared spectroscopy (FTIR) is widely used for the rapid and non-destructive characterization of the macromolecule structures (lipids, proteins, nucleic acids, and polysaccharides) [39]. More specifically, amongst the various techniques used, attenuated total micro reflectance (ATR) is viewed as very advantageous as it doesn't require any sample preparation prior to spectral analysis. In ATR measurements, the depth of penetration of the IR radiation into the sample is independent of the sample thickness. Consequently, by layering the solid sample directly on the micro diamond crystal, structural information at different parts of the sample may be gained. Specifically, it was used to identify species and geographic origin of *Boletus* sp. mushrooms [40] or quantify the total polysaccharide content in *Ganoderma* mycelia [41], as well as glucans and ergosterol content in *Pleurotus* [42]. In an earlier study, it was also used to show how physical harm had an effect on tissue structure and the aging process [43]. The most intriguing application of this technique is currently the degradation processes of various agricultural waste for mushroom cultivation [44,45].

To this aim, *G. lucidum*, *L. edodes*, and *P. cornucopiae* were grown on HS substrates in order to evaluate their potential as alternative growth substrates. In order to accomplish this objective, mycelia growth rate and biological efficiency were studied. Additionally, micro ATR-FTIR was applied to explore the substrate breakdown and the composition of the fruiting bodies.

2. Materials and Methods

2.1. Substrates

The hazelnut shells were provided by an organic farm located in Carrù (Cuneo, Piedmont, Italy). Wheat straw (WS) and *Fagus* sp. L. chips (Beech Chips, BC) were kindly provided by the Cadriano farm of the University of Bologna. Wheat straw and BC were crushed into fragments smaller than 0.5 cm; HS was crushed with a cutting mill (Retsch, SM 100) and autoclaved at 121 ± 1 °C for 60 min to prevent any contamination during storage. The dried raw materials were stored at 22 ± 1 °C.

2.2. Mushrooms Cultures and Mycelial Growth Rate Evaluation

Experimental trials were carried out by using three species of Basidiomycetes mushrooms: *G. lucidum*, *L. edodes*, and *P. cornucopiae*.

Ganoderma lucidum (strain Glu16) and *P. cornucopiae* (strain Pco3) were isolated from fruiting bodies collected in the wild; *L. edodes* strain (LEd5) was brought by the Fungal Institute of Jinxiang (Shandong province, China).

The mycelial pure cultures were stored in the Mycological and Applied Botany Laboratory of the Department of Agricultural and Food Sciences (DISTAL) at the University of Bologna (Bologna, Italy). The isolates were kept at 22 ± 1 °C in darkness on Potato Dextrose Agar (PDA, Difco) half strength and subcultured every two months.

For mycelial growth area evaluation, plugs of 10 mm diameter were taken by 15-day-old colonies of each species and inoculated in the center of 9 cm sterilized Petri dish filled with 30 g of three different substrates previously soaked for 24 h with distilled water and brought to 70% humidity: Hazelnut Shell (HS); Wheat Straw 50%-Hazelnut Shell 50% (WS 50%-HS 50%) and Wheat Straw (WS) as control. Five replicates were made for each combination of species and substrate. All plates were incubated at 22 ± 1 °C in darkness. The fungal growth was assessed by measuring the diameter of the colony along two preset diametrical lines every day.

The area (cm^2) covered daily by the mycelium was calculated assuming an elliptical shape as reported by [46] using the following formula:

$$A = \pi \times R_1 \times R_2$$

where A is the fungal colony area (cm^2) and R_1 and R_2 are the two perpendicular radii, respectively.

The area growth rate of the mycelium (*AGR*) was calculated with the formula of Sinclair and Cantero [47] modified as follows:

$$AGR = \frac{A_f - A_i}{T_f - T_i}$$

where *AGR* is the growth rate (cm^2 day^{-1}); A_f is the final growth area (cm^2); A_i is the initial growth area (cm^2) and T_f is the final growth time (days); T_i is the initial growth time (days).

2.3. Mushrooms Cultivation Trials

Spawn production occurs in inoculated glass tubes containing 30 g of sorghum kernels and distilled water in a 1:2 (v/v) ratio, previously sterilized at 121 ± 1 °C for 20 min, with two 15-day-old mycelial plugs of 1 cm diameter. Five replicates were prepared for each species-substrate combination. The tubes were incubated in the dark at 22 ± 1 °C for 30 days with the aim to obtain the complete colonization of the kernels.

Two different HS-based substrates were used as reported in Table 1; a substrate composed of wheat straw 50% and Beech Chips 50% was used as a control. Homogeneous substrate mixtures were prepared by mixing component materials based on their dry weight (w/w).

Table 1. Composition and ratios of the substrates used in cultivation trials.

Substrates and Mixing Ratio	Code	Average Dry Weight (g)
Wheat Straw 50%-Beech Chips 50% (control)	WS-BC	400
Wheat Straw 50%-Hazelnut Shells 50%	WS-HS	900
Hazelnut Shells 100%	HS	1500

The substrates were inserted into autoclavable polypropylene (PP) transparent bags (20 × 30 cm). Dried mixed substrates were moistened with 1 L (per bag) of distilled water for 24 h and the excess of water was removed by squeezing the bags.

Bags were closed with a PP plastic cap with a filter, autoclaved at 121 ± 1 °C for 60 min; inoculated with grain spawn by opening the bag, inserting the inoculum inside it (1 tube per bag), mixing the inoculum with the substrate, and incubated in the darkness at 22 ± 1 °C until the complete colonization of the substrate. For each species-substrate combination, five bags were prepared.

After 1 or 2 months of mycelial growth, depending on the substrate (one month on WS and WS-BC and around 2 month on HS), bags were moved to a climatic chamber with different climatic conditions (Table 2) according to their biological needs [48].

Table 2. Cultivation parameters used in the trials.

	Species		
	Ganoderma lucidum	*Lentinula edodes*	*Pleurotus cornucopiae*
Temperature (°C)	22–30	10–20	18–25
Light intensity (Lux)	500–1000	500–1000	500–1000
Relative Humidity (%)	85–95	60–95	80–95

Lentinula edodes fruiting body were collected only when the cap radius reached 5 cm in diameter [49]. *Ganoderma lucidum* and *P. cornucopiae* were collected when the cap was completely developed. The duration of the harvest periods, starting from the appearance of the first primordia, was two months for *L. edodes* and *P. cornucopiae* and 3 months for *G. lucidum*. All fruiting bodies were freshly weighted, dried in a stove at 40 °C for 24 h, and their dried weight was recorded. Biological efficiency was calculated according to Chang et al., 1981 [50].

2.4. Micro ATR-FTIR Spectroscopy Analysis

A Bruker Tensor FT-IR instrument (Bruker Optics, Ettlingen, Germany) equipped with an accessory for analysis in ATR was used. The sampling device contained a micro-diamond crystal, single reflection with an angle of incidence of 45° (Specac Quest ATR, Specac Ltd., Orpington, Kent, UK). Spectra were recorded from 4000 to 400 cm^{-1}, with a spectral resolution of 4 cm^{-1} and 64 scans. Background spectra were also taken against air under the same conditions before each sample.

The substrates from in vitro test were analyzed after 30 days of mycelial growth, as previously described by Fornito et al., 2020 [44]. Parts of dried fruiting bodies (cap, hymenophore, and stipe) grown on the HS and WS-BC of each species were placed on the diamond crystal, and pressure was applied with a compression clamp. The resulting spectra of each type of sample were averaged. Isopropyl alcohol was used to clean the diamond crystal before each recording.

2.5. Statistical Analyses

Statistical analyses were performed using the RStudio [51] graphical interface for the R software environment v.4.0.2 (R Foundation, Vienna, Austria) with the packages agricolae, ggplot2, Hmisc, and mice. The analysis of variance (ANOVA) and Kruskal-Wallis test were used to determine the significant difference of AGR, Fruiting body production (FBP, expressed as dry weight of mushrooms collected during the harvesting period), and biological efficiency among different substrates. Tukey post hoc test ($p \leq 0.05$) was used to compare the means.

3. Results

3.1. In Vitro Mycelial Growth and ATR-FTIR of Substrates

Figure 1 shows the in vitro mycelial growth of the tested fungi in the three different substrates. Only *P. cornucopiae* showed a significantly higher mycelial growth rate on WS (Figure 1e,f). The growth of *G. lucidum*, *L. edodes*, and *P. cornucopiae* was significantly lower on HS with respect to the other substrates (Figure 1a,c,e). Statistical differences were found

between the area growth rate of *G. lucidum* and *L. edodes* grown on HS respect to WS and WS-HS (Figure 1b,d).
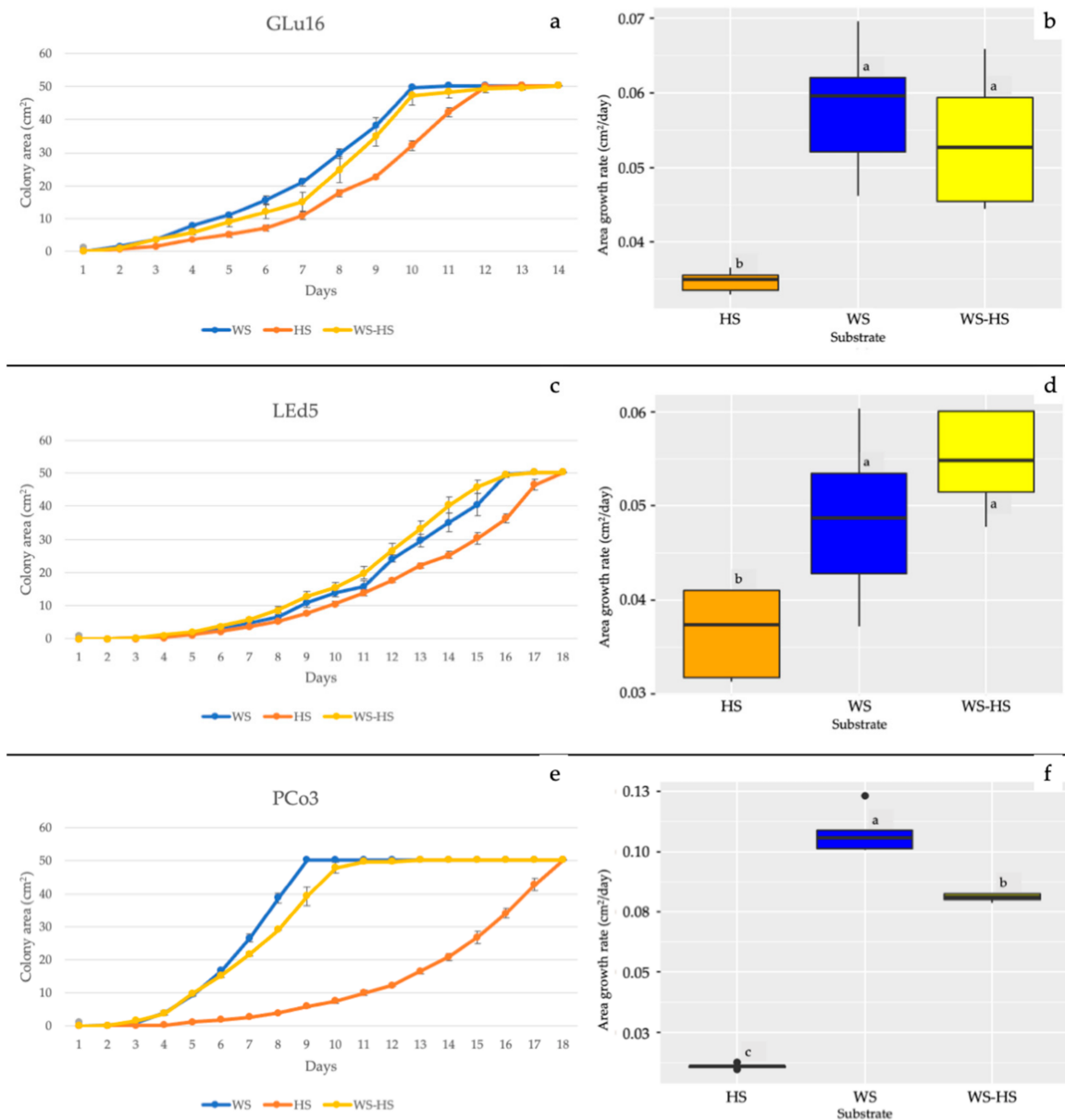

Figure 1. Growth and AGR of (**a**,**b**) *Ganoderma lucidum*, (**c**,**d**) *Lentinula edodes,* and (**e**,**f**) *Pleurotus cornucopiae* in Petri dishes on WS (blue), HS (orange), and WS-HS (yellow). Different letters indicate significant differences at $p \leq 0.05$.

In the fingerprint region (1800–600 cm^{-1}) of the substrate spectra, WS and HS, and after 30 days of mycelial growth, consistent structural variation for both substrates were found for *G. lucidum*, *L. edodes,* and *P. cornucopiae* (Figure 2a,b). In the WS spectrum (black line) (Figure 2a), the bands at 1735 cm^{-1}, due to unconjugated C=O, and at 1460 cm^{-1} (C–H deformation), correspond to those of xylan (hemicellulose) or the heterocyclic cellulosic rings [52]. The peak at 1623 cm^{-1} may be assigned to carboxylates in aromatic rings. The shoulder at 1517 cm^{-1} was attributed to the aromatic skeletal vibrations (C=C) and aromatic breathing in lignin, respectively [53–55]. The bands at 1423 cm^{-1} and 1322 cm^{-1} were assigned to C–H$_2$ bending at C-6 of the crystalline cellulose [56], and that at 1370 cm^{-1} was due to CH$_2$ bending vibrations in cellulose and hemicellulose. The region between 1100 and 950 cm^{-1} corresponded to that of cellulose and hemicelluloses. The most intense

bands centered at 1031 cm^{-1} were assigned to the C–O–C stretching of primary alcohol in cellulose and hemicellulose [57]. The weak shoulder at 898 cm^{-1} was associated with C1–O–C β-(1–4)-glycosidic linkage in cellulose. The other bands at approximately 700 cm^{-1} and 600 cm^{-1} were assigned to the C–OH bending [58,59].
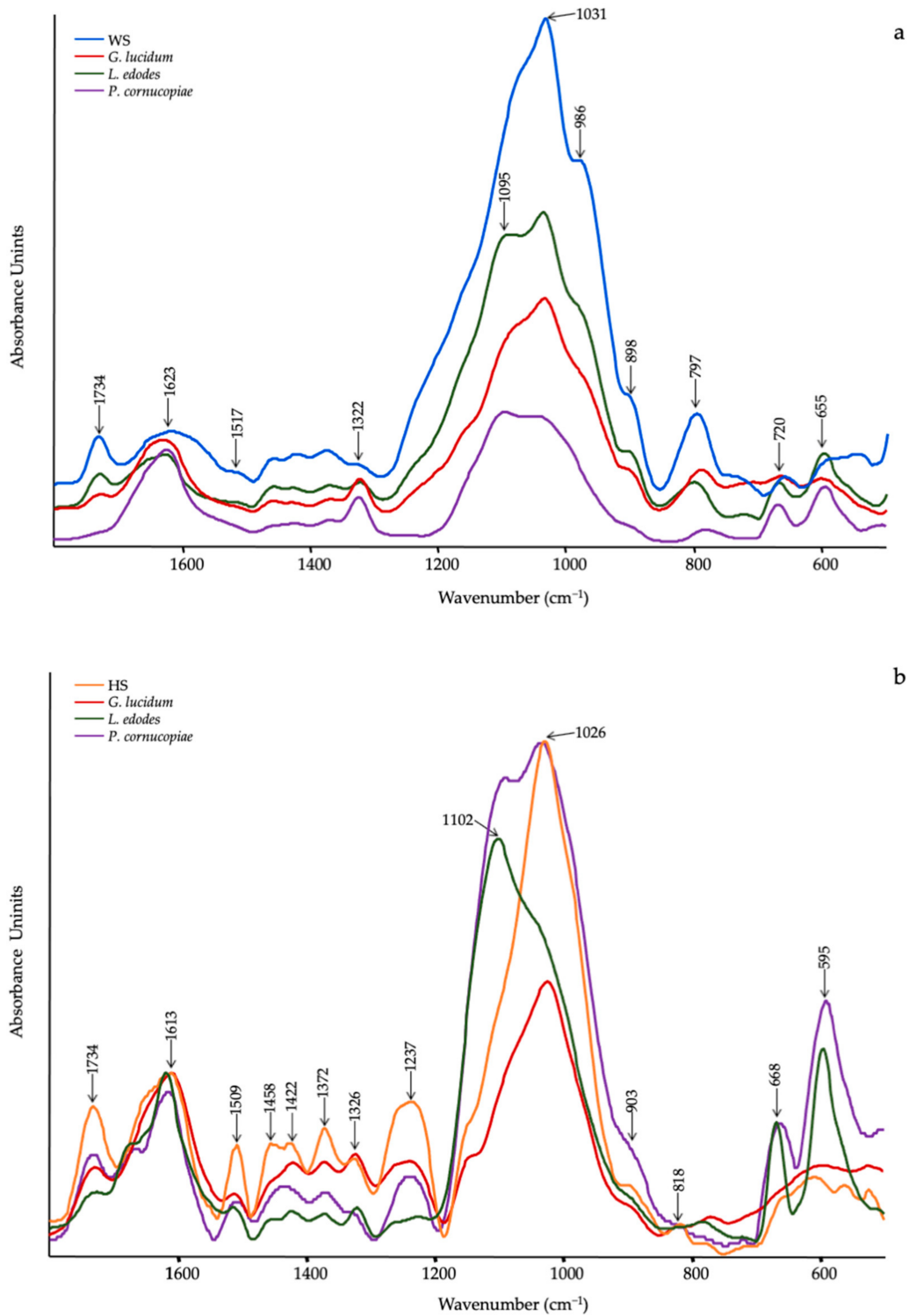

Figure 2. ATR-FTIR spectra of (**a**) WS (blue line) and (**b**) HS (orange line) after 30 d of mycelial growth of *G. lucidum* (red line), *L. edodes* (green line) and *Pleurotus cornucopiae* (purple line).

After 30 days of mycelial growth, a considerable structural modification was observed. In particular, the progressive decrease of xylan in hemicellulose (1735 cm^{-1} and 1460 cm^{-1}) in *L. edodes* and *G. lucidum* and the total disappearing in *P. cornucopiae* was observed in the spectra (Figure 2a).

Lignin decay may be ascertained in the decreased intensity of absorption bands at around 1623 cm^{-1}, appearing more significant in *P. cornucopiae*. Conversely, the band at 1322 cm^{-1} (Figure 2a) increased in *G. lucidum* and *P. cornucopiae*. More significant variations were also observed in the glycosidic C–O–C band (1100–950 cm^{-1}), showing an alteration of the linkage C1–O–C β-(1–4)-sugar of the polymeric cellulose in the following order: *P. cornucopiae* > *G. lucidum* > *L. edodes*, probably as a result of cellulose degradation processes. As shown in Figure 2b, the HS spectrum (blue line) displayed a number of adsorption peaks, indicating the complex nature of the material examined [60]. More precisely, the peak centered at 1734 cm^{-1} could be ascribed to acetyl and uronic ester groups in hemicellulose and ρ-coumaric acids in lignin [40]. The bands at 1613 cm^{-1} and 1509 cm^{-1} corresponded to the aromatic skeletal vibration in lignin [52] as well as the bands at 1458 cm^{-1}. In addition, the bands at 1422 cm^{-1} were derived from C–H bending in lignin. The cellulose and hemicellulose bands appeared at 1372 cm^{-1} and 1326 cm^{-1} (C–H bending). Nevertheless, the last band also may be assigned to C–O vibration in syringyl derivatives as well as the band at approximately 1237 cm^{-1}, due to syringyl ring and C–O stretching in lignin and xylan [60]. The most intense region from 1100 to 900 cm^{-1} was attributed to C–O and C–O–C stretching in cellulose and hemicellulose. Spectra after mycelia growth showed a progressive reduction in the relative intensity of the aromatic rings (1509 cm^{-1}, 1326 cm^{-1}, and 1237 cm^{-1}) in this order: *L. edodes* > *G. lucidum* > *P. cornucopiae*. Likewise, the gradual decrease in the peak at 1734 cm^{-1} might be related to the presence of ρ-coumaric acids from the lignin rather than the hemicellulose. In the region corresponding to cellulose and hemicelluloses (1100 to 900 cm^{-1}), a significant increase in C–O (1102 cm^{-1}) group in *P. cornucopiae* and *L. edodes* was detected. On the contrary, the C−O−C group decreased in *G. lucidum* and *L. edodes* (Figure 2b).

3.2. Fruiting Body Production

In Figure 3, the FBP and the biological efficiency of all the tested fungi in different substrates are reported. The FBP of *L. edodes* was significantly higher on HS than on the other tested substrates (Figure 3c). The *P. cornucopiae* FBP on HS was significantly higher than on WS-BC but had similar production as on WS-HS (Figure 3e). In contrast, the FBP of *G. lucidum* was significantly lower in HS than WS-BC but similar to FBP on WS-HS (Figure 3a). Regarding the biological efficiency, all the tested fungi showed a higher biological efficiency on WS-BC with respect to the other substrates (Figure 3b,d,f).

3.3. Qualitative Evaluation of Mushrooms by ATR-FTIR

The spectra of the fruiting bodies of *G. lucidum*, *L. edodes*, and *P. cornucopiae* produced on different growing media (HS and WS-BC) are shown in Figure 4.

As no spectral difference from 1800 cm^{-1} to 800 cm^{-1} was detected between the cap, the gills, and the stipe in either *L. edodes* or *P. cornucopiae*, the spectra were averaged (Figure 4a,b). Conversely, in the *G. lucidum* spectra, a significant spectral variation was observed between the cap and the hymenophore (Figure 4c,d). The characteristic bands of the main functional groups are listed in Table 3.
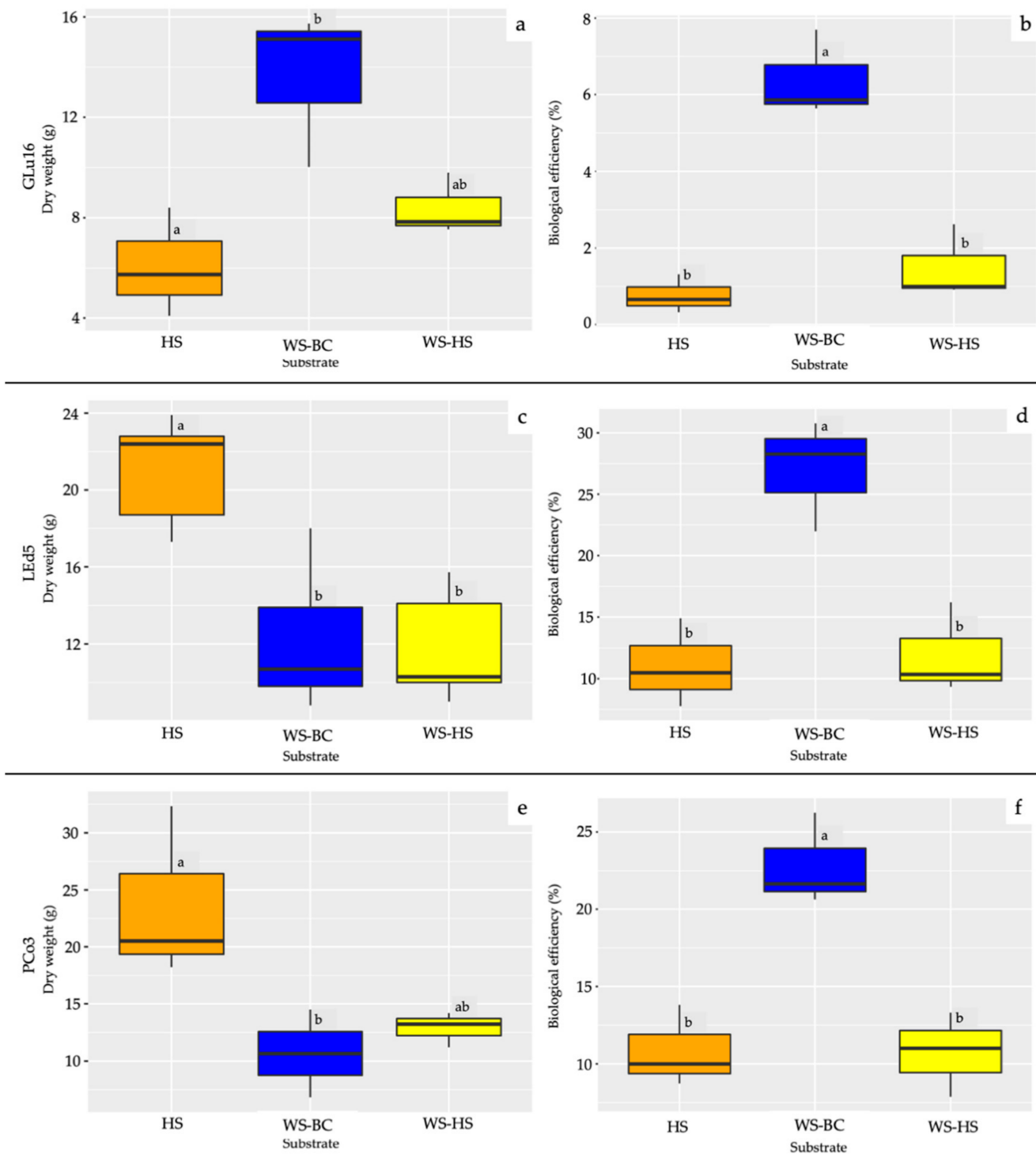
Figure 3. FBP and biological efficiency of (**a**,**b**) *Ganoderma lucidum*; (**c**,**d**) *Lentinula edodes*, and (**e**,**f**) *Pleurotus cornucopiae* grown on HS (orange), WS-BC (blue), and WS-HS (yellow). Different letters indicate significant differences at $p \leq 0.05$.
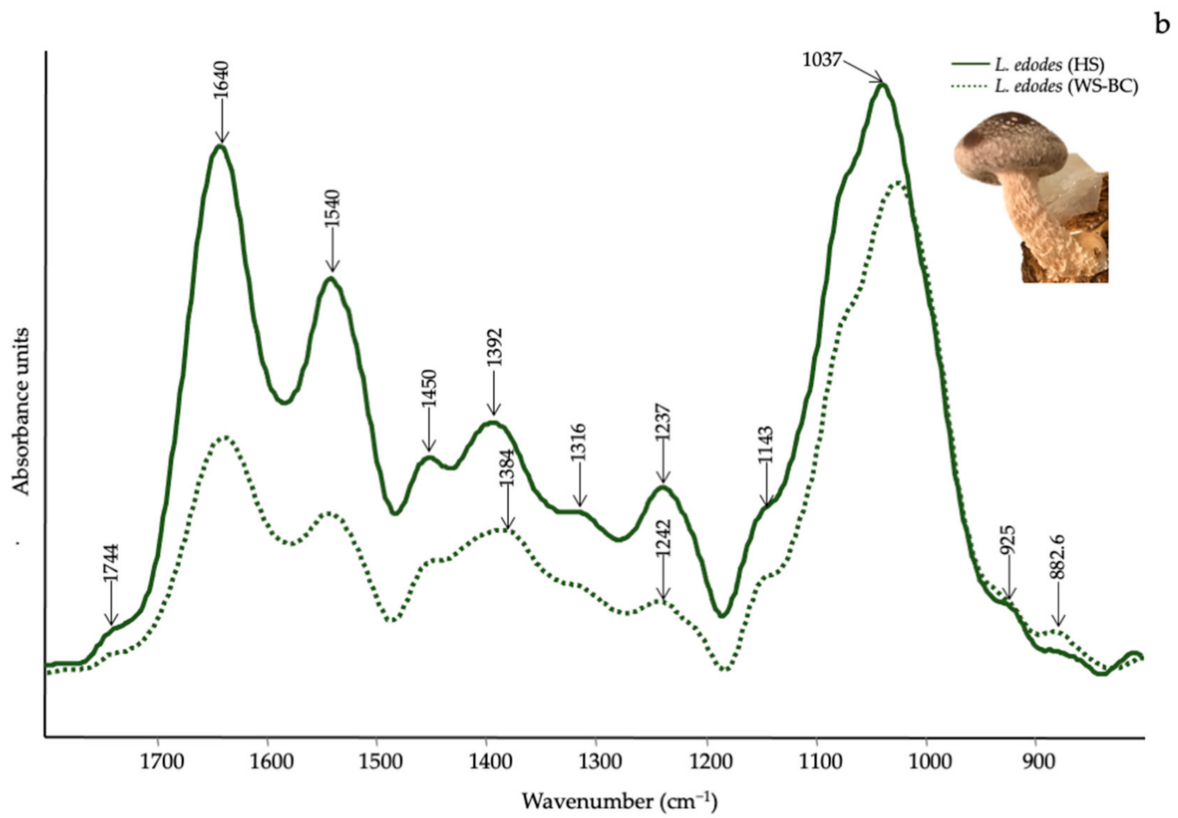
Figure 4. *Cont.*

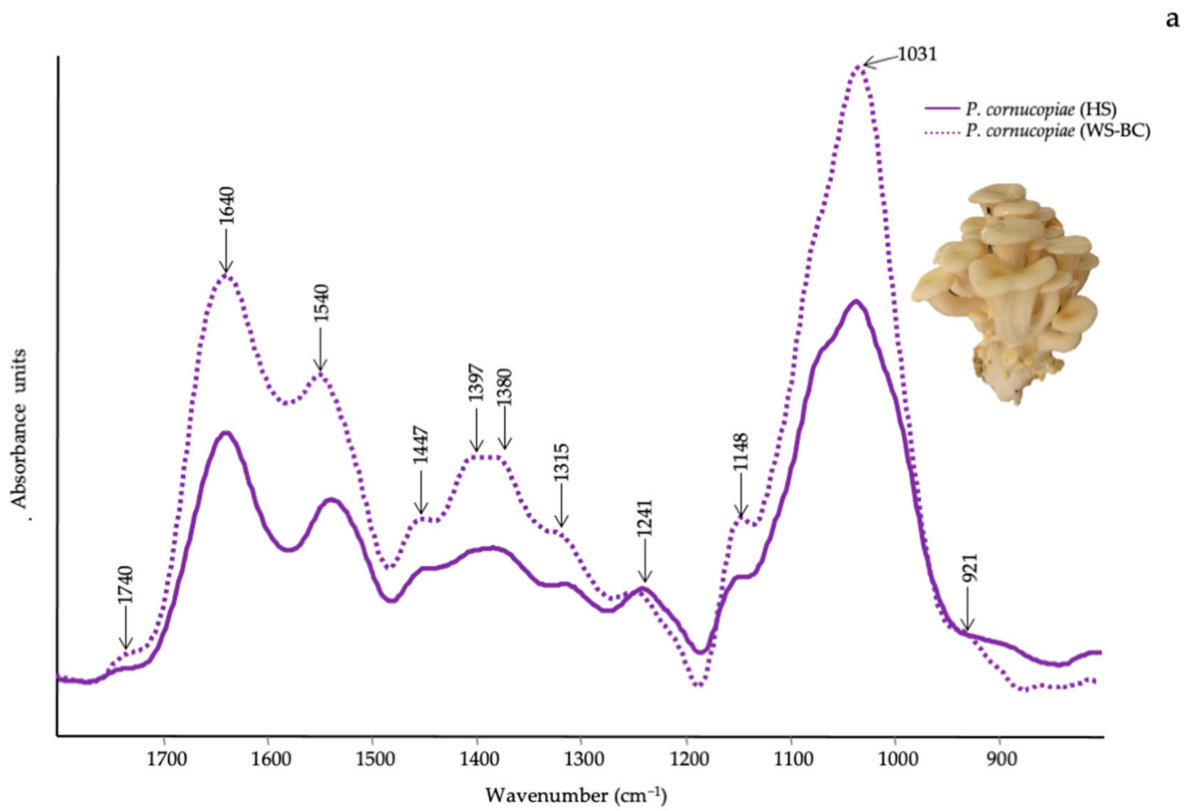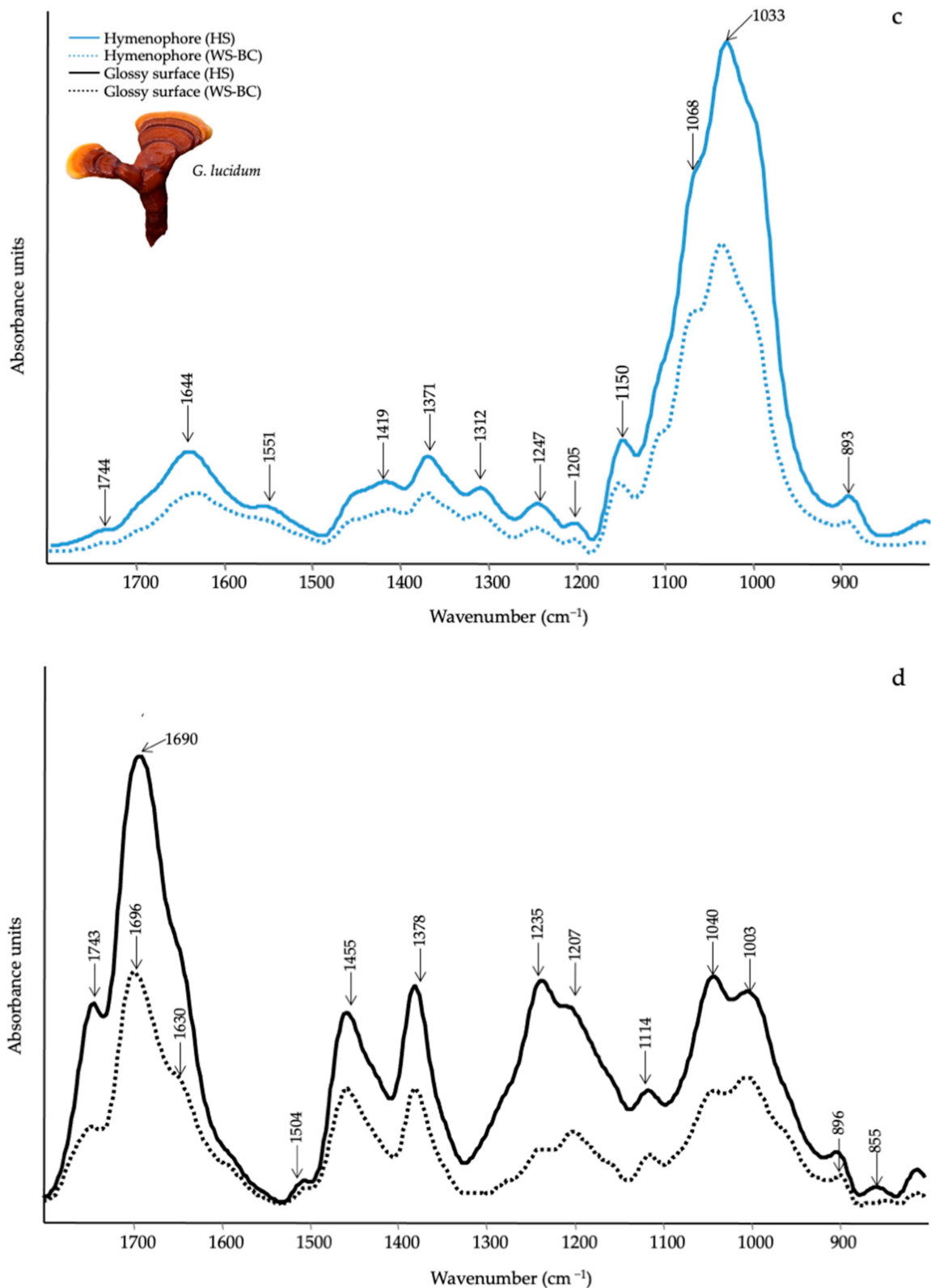**Figure 4.** ATR-FTIR spectra of the fruiting bodies of (**a**) *P. cornucopiae* cultivated on WS-BC (dotted purple line) and HS (solid purple line); (**b**) *L. edodes* cultivated on WS-BC (dotted green line) and HS (solid green line); (**c**) *G. lucidum* hymenophore on WS-BC (dotted cyan line) and HS (solid cyan line); (**d**) *G. lucidum* glossy surface on WS-BC (dotted black line) and HS (solid black line).

Table 3. Attributions of the main characteristic FT-IR bands in the spectra of *G. lucidum*, *L. edodes* and *P. cornucopiae* fruiting bodies according to the literature.

Wavenumber (cm^{-1})	Functional Groups Attributions	Reference
1745–1738	C=O stretching of lipids	[61]
1696–1690	CHO stretching in aromatic	[62]
1640–1638	Amide I, water	[61]
1540–1548	Amide II	[61]
1507	Aromatic ring	[62]
1455	CH$_2$ bending in polysaccharides	[39]
1400–1378	C–H in-plane bending vibration	[63]
1245–1235	Amide III and C–O stretching	[40]
1150–1157	C–O–C asymmetric stretching of glycosidic linkage	[43]
1040–1025	stretching vibration of C–O–C group	[43]
930–882	Glucan band β anomer; C–H deformation	[64]
807–796	α (1–6) linked backbone with α (1–3); CH out-of plane bending	[64]

In the spectra of *P. cornucopiae* and *L. edodes* (Figure 4a,b) are well identifiable the Amide I (~1640 cm^{-1}), Amide II (~1540 cm^{-1}) and Amide III (~1240 cm^{-1}) bands of proteins [61]. Another characteristic is valuable in the region of polysaccharides vibrations between 1150–796 cm^{-1} (Table 3). More specifically, the bands at about 807 cm^{-1} and 930 cm^{-1} are corroborating for mannan [α (1-6) linked backbone with α (1-3) and α (1-2) linked branches] a type of glucan that is one component of fungal cell walls and chitin (N-acetylglucosamine based polymer), respectively [64]. A weak shoulder at around 1740 cm^{-1} indicated the presence of cell membrane phospholipids [61]. *Pleurotus cornucopiae* grown on WS-BC and HS (Figure 4a) showed a similar spectral profile, although an increase in the relative intensity of the bands was seen in presence of WS-BC and more specifically, in the polysaccharide region. At the opposite, the spectra of *L. edodes* grown on HS consistently showed an increase in the relative intensity of all bands as compared to the WS-BC substrate (Figure 4b). However, no relevant structural variation was observed.

Referring to the spectra of *G. lucidum* grown on HS and WS-BC, a different spectral profile was detected both in the external and inner parts of the fruiting body and in the different substrate (Figure 4c,d). The glossy surface part of both cap and stipe were characterized by esterified carboxyl groups in lipids at 1745 cm^{-1} and 1235 cm^{-1}, respectively. These bands may also be coupled to vibrations at 1455 cm^{-1} and 1378 cm^{-1} in C–H bending of aliphatic compounds. The band at 1690 cm^{-1}, 1630 cm^{-1}, and 1504 cm^{-1} were due to aromatic rings vibrations [62]. The region from 1100 to 896 cm^{-1} belonged to the vibration of C–C–O or C–C–OH in polysaccharides (Table 3). In the inner part of the fruiting body and hymenophore, the lipid functional groups (1744 cm^{-1}, 1450 cm^{-1}, 1371 cm^{-1} and 1247 cm^{-1}) become weaker (Figure 4c) than those observed in the surface. Instead, the bands of amide I, (1644 cm^{-1}) and amide II (1551 cm^{-1}) were visible. The spectra were also dominated by the intense bands assigned to polysaccharides from 1150 to 893 cm^{-1}. By comparing the spectra of *G. lucidum* grown on HS and WS-BC, the main variations occurred in the polysaccharide region, which appeared more intense in HS than in WS-BC.

4. Discussion

The circular economy in the agro-wastes management sector requires reusing these materials as a feedstock in a variety of production cycles. In this context, the high production of hazelnuts has led to a significant accumulation of wood residues frequently involved in manufacturing processes, potentially impacting the environment.

In this work, we explored the potential of HS as a growing substrate for the cultivation of edible and medicinal mushrooms.

Preliminary results in Petri dishes indicated that all the three tested species were able to grow on HS (Figure 1), which was never used for mushroom cultivation.

It is well known that the C/N ratio is one of the most important parameters for mushroom growth and cultivation [65]. The C/N ratio of hazelnut shells ranged from 43.4 to 58 [66–68]; this C/N ratio is optimal for *L. edodes* and *P. cornucopiae* and sub-optimal for *G. lucidum.* In fact, the optimal C/N ratio for *L. edodes* and *P. cornucopiae* ranges from 30–35 and 45–55, respectively, whereas *G. lucidum* development is favored by C/N ratios between 70 and 80 [48,68].

All the tested species are considered white-rot fungi naturally found on hardwood [69]. However, *G. lucidum*, *L. edodes,* and *P. cornucopiae* showed a different behavior on the tested substrates. *Pleurotus cornucopiae* grow better on WS and WS-HS with respect to HS (Figure 1e,f), this different behavior could be due to the different lignin percentage in HS (ranging from 40 to 50%) [5–7] with respect to WS (15%) [70,71] and the greater presence of soluble sugars and nutrients present in WS. In fact, *P. cornucopiae* on WS and WS-HS rapidly covered the surface of the plate and then degraded its cellulose and available hemicellulose. In contrast, in HS substrate, lesser soluble nutrients were released, and lesser cellulose and hemicellulose were available without previous degradation of lignin. Moreover, *P. cornucopiae* is typically found on poplar wood which contains a percentage of lignin ranging from 16 to 21% [72]. On the other hand, *G. lucidum* and *L. edodes* are commonly found on oaks and on chestnut trees, whose lignin content ranging from 18–30% in oak wood to 26% in chestnut wood [73,74].

The efficiency of mycelial growth on different substrates may be related to the structural modification detected in the spectra (Figure 2a,b). Since the lignocellulose is the major component of any substrate, the changes observed in the spectra presumed a synergistic action of several enzymes [68,75]. As expected, the mycelial growth of *P. cornucopiae* in WS-BC resulted in a change in the acetyl and uronic ester groups of hemicellulose (1734 cm^{-1}) and in those bound to the C1–O–C β-(1-4)-sugar bond of cellulose. Based on these structural changes, we can surmise that enzymatic hydrolysis led to a total degradation of β-(1,4) glycosidic bonds with the missing band at 898 cm^{-1} and the production of new simple molecules, most likely as sugar acids (Figure 2a). Substrate degradation activity by *G. lucidum* and *L. edodes* did not lead to significant structural changes in WS-BC, even though in *G. lucidum* is visible light degradative activity of acetyl and uronic ester groups of hemicellulose (1734 cm^{-1}).

As previously reported, the higher mycelia growth capacity of *G. lucidum* and *L. edodes* on HS could be related with the high lignin, cellulose, and hemicellulose contents. Specifically, *G. lucidum* caused a modification of the HS substrate with reduction of the acetyl and uronic ester groups of hemicellulose (1734 cm^{-1}) and of those linked to the C1–O–C β-(1-4)-sugar bond of cellulose. In addition, the typical lignin aromatic ring (1509 cm^{-1}) showed consistent degradation that, coupled with the gradual decrease of the peak at 1734 cm^{-1} related to ρ-coumaric acids rather than to hemicellulose, suggests that lignin degradation is the first level of lignocellulose degradation in order that cellulose and hemicellulose accessibility is more feasible [76]. With *L. edodes* and *P. cornucopiae,* the alterations were mainly related to the region of cellulose and hemicelluloses (1100 to 900 cm^{-1}). The increase in these bands may indicate that a variety of hydrolytic enzymes could be released during fungal attacks specifically to modify and break the bonds of the lignin and hemicellulose; the chemical changes in these compounds signal that the fungus could take them as carbon sources.

After in vitro preliminary tests, cultivation trials conducted on *G. lucidum*, *L. edodes*, and *P. cornucopiae* showed a biological efficiency on HS (0.8, 11.0, and 10.8%, respectively) lower than those obtained on WS-BC (6.4, 21.9, and 22.9%, respectively), but the biological efficiency on WS-BC are in line with those previously obtained by other authors [77–79]. The lower biological efficiency on HS could be attributed to the higher dry weight of the substrate used to fill each bag. *Lentinula edodes* and *P. cornucopiae* showed a good FBP, proving capable of exploiting HS-based substrates, although the growth of *P. cornucopiae* in vitro was slower than WS and WS-HS. In contrast, *G. lucidum* had a lower FBP on HS despite rapid development in vitro. The mycelial colonization and the fruiting body

production could not be strictly correlated as in not ideal substrates; several fungi show a faster colony expansion for a foraging strategy [80].

A spectroscopic comparison of *P. cornucopiae* fruiting bodies grown on WS-BC displayed a higher content in polysaccharide than those on HS (Figure 4a). The higher biosynthesis of polysaccharides in *P. cornucopiae* is strongly influenced by the chemical composition of the substrates, and in particular, by cellulose and hemicellulose availability as also claimed by Bekiaris, 2020 [42]. Conversely, in *L. edodes* grown on HS, polysaccharides increased, chitin in particular, confirming the role of the substrate composition. It is known that *L. edodes* grown on a wood log have a greater economic value than those grown on WS for their better quality [81]. Our preliminary sensory data showed that the fruiting bodies of *L. edodes* grown on HS have a better texture, probably due to the higher chitin content [82], aroma, and color than those grown on WS-BC (data not shown). These differences could be due to the high lignin content present in HS, which could provide a fruiting body qualitatively similar to those obtained on wood logs. This result also suggests that a high chitin and polysaccharide content in the *L. edodes* fruiting bodies could be an indicator of the quality of its fruiting bodies. On the other hand, differences in the chemical composition of the medicinal mushroom *G. lucidum* were found both on the glossy surface and in the inner part of the fruiting bodies grown on WS-BC and HS. It is confirmed that the HS substrate led to the enhancement of polysaccharides with respect to those grown on WS-BC. Polysaccharides are the most biologically active substances in *G. lucidum* endowed with antitumor, antiviral, antioxidant, and immunomodulatory activities and for medicinal uses of *Ganoderma* spp. the Chinese Pharmacopoeia has established a minimum content of polysaccharides in the dry fruiting body [35].

5. Conclusions

The high demand for hazelnuts and their consequent use in the food industry leads to an accumulation of woody biomass consisting of HS. The valorization of HS as a substrate for mushroom cultivation is an environmentally friendly alternative to the conventional utilization of such agricultural waste by-products.

The results obtained in this study support the economic applicability of HS as a substrate or supplement for mushroom cultivation according to circular economy criteria and in order to obtain high-quality food. The high lignin content of HS makes it an appropriate substrate for mushroom cultivation, resulting in greater optimization of this agricultural waste by-product and, consequently, more profit for mushroom farms. In addition, at the end of the fungal growth cycle, the spent mushroom substrate after lignocellulosic degradation may also be used to improve soil fertility by supplying beneficial nutrients for crops.

Author Contributions: Conceptualization, F.P. and P.L.; methodology, O.F.; validation, P.L. and F.M.; formal analysis, P.L. and F.M.; investigation, F.P., P.L. and F.M.; resources, A.Z. and O.F.; data curation, P.L. and F.M.; writing—original draft preparation, F.P.; writing—review and editing, A.Z. and O.F.; visualization, F.P.; supervision, A.Z. and O.F. All authors have read and agreed to the published version of the manuscript.

Institutional Review Board Statement: Not applicable.

Informed Consent Statement: Not applicable.

Data Availability Statement: The data presented in this study are available on request from the corresponding author.

Conflicts of Interest: The authors declare no conflict of interest.

References

1. Food and Agricultural Organization of the United Nations. FAOSTAT. Available online: https://www.fao.org/faostat/en/#data/QCL (accessed on 15 December 2021).
2. Król, K.; Gantner, M. Morphological traits and chemical composition of hazelnut from different geographical origins: A review. *Agriculture* **2020**, *10*, 375. [CrossRef]
3. Silvestri, C.; Bacchetta, L.; Bellincontro, A.; Cristofori, V. Advances in cultivar choice, hazelnut orchard management, and nut storage to enhance product quality and safety: An overview. *J. Sci. Food Agric.* **2021**, *101*, 27–43. [CrossRef]
4. Król, K.; Gantner, M.; Piotrowska, A. The quality characteristic and fatty acid profile of cold-pressed hazelnut oils during nine months of storage. *Agronomy* **2021**, *11*, 2045. [CrossRef]
5. Rivas, S.; Moure, A.; Parajó, J.C. Pretreatment of hazelnut shells as a key strategy for the solubilization and valorization of hemicelluloses into bioactive compounds. *Agronomy* **2020**, *10*, 760. [CrossRef]
6. Pérez-Armada, L.; Rivas, S.; González, B.; Moure, A. Extraction of phenolic compounds from hazelnut shells by green processes. *J. Food Eng.* **2019**, *255*, 1–8. [CrossRef]
7. Hoşgün, E.Z.; Bozan, B. Effect of different types of thermochemical pretreatment on the enzymatic hydrolysis and the composition of hazelnut shells. *Waste Biomass Valorization* **2020**, *11*, 3739–3748. [CrossRef]
8. Guney, M.S. Utilization of hazelnut husk as biomass. *Sustain. Energy Technol. Assess.* **2013**, *4*, 72–77. [CrossRef]
9. Arslan, Y.; Takaç, S.; Eken-Saraçoğlu, N. Kinetic study of hemicellulosic sugar production from hazelnut shells. *Chem. Eng. J.* **2012**, *185–186*, 23–28. [CrossRef]
10. Özçelik, E.; Pekşen, A. Hazelnut husk as a substrate for the cultivation of shiitake mushroom (*Lentinula edodes*). *Bioresour. Technol.* **2007**, *98*, 2652–2658. [CrossRef]
11. Uzuner, S.; Sharma Shivappa, R.R.; Cekmecelioglu, D. Bioconversion of alkali pretreated hazelnut shells to fermentable sugars for generation of high value products. *Waste Biomass Valorization* **2017**, *8*, 407–416. [CrossRef]
12. Çöpür, Y.; Güler, C.; Taşçıoğlu, C.; Tozluoğlu, A. Incorporation of hazelnut shell and husk in MDF production. *Bioresour. Technol.* **2008**, *99*, 7402–7406. [CrossRef] [PubMed]
13. Barbu, M.C.; Sepperer, T.; Tudor, E.M.; Petutschnigg, A. Walnut and hazelnut shells: Untapped industrial resources and their suitability in lignocellulosic composites. *Appl. Sci.* **2020**, *10*, 6340. [CrossRef]
14. Şencan, A.; Karaboyacı, M.; Kılıç, M. Determination of lead(II) sorption capacity of hazelnut shell and activated carbon obtained from hazelnut shell activated with ZnCl₂. *Environ. Sci. Pollut. Res.* **2015**, *22*, 3238–3248. [CrossRef] [PubMed]
15. Cimino, G.; Passerini, A.; Toscano, G. Removal of toxic cations and Cr(VI) from aqueous solution by hazelnut shell. *Water Res.* **2000**, *34*, 2955–2962. [CrossRef]
16. Kazemipour, M.; Ansari, M.; Tajrobehkar, S.; Majdzadeh, M.; Kermani, H.R. Removal of lead, cadmium, zinc, and copper from industrial wastewater by carbon developed from walnut, hazelnut, almond, pistachio shell, and apricot stone. *J. Hazard. Mater.* **2008**, *150*, 322–327. [CrossRef]
17. Kobya, M.; Demirbas, E.; Öncel, M.S.; Sencan, S. Adsorption kinetic models applied to nickel ions on hazelnut shell activated carbons. *Adsorpt. Sci. Technol.* **2002**, *20*, 179–188. [CrossRef]
18. Demirbas, E.; Dizge, N.; Sulak, M.T.; Kobya, M. Adsorption kinetics and equilibrium of copper from aqueous solutions using hazelnut shell activated carbon. *Chem. Eng. J.* **2009**, *148*, 480–487. [CrossRef]
19. Sert, S.; Çelik, A.; Tirtom, V.N. Removal of arsenic(III) ions from aqueous solutions by modified hazelnut shell. *Desalin. Water Treat.* **2017**, *75*, 115–123. [CrossRef]
20. Pehlivan, E.; Altun, T.; Cetin, S.; Iqbal Bhanger, M. Lead sorption by waste biomass of hazelnut and almond shell. *J. Hazard. Mater.* **2009**, *167*, 1203–1208. [CrossRef]
21. Demirbaş, E. Adsorption of cobalt(II) ions from aqueous solution onto activated carbon prepared from hazelnut shells. *Adsorpt. Sci. Technol.* **2003**, *21*, 951–963. [CrossRef]
22. Lewicka, K. Activated carbons prepared from hazelnut shells, walnut shells and peanut shells for high CO₂ adsorption. *Polish J. Chem. Technol.* **2017**, *19*, 38–43. [CrossRef]
23. Contini, M.; Baccelloni, S.; Massantini, R.; Anelli, G. Extraction of natural antioxidants from hazelnut (*Corylus avellana* L.) shell and skin wastes by long maceration at room temperature. *Food Chem.* **2008**, *110*, 659–669. [CrossRef]
24. Yuan, B.; Lu, M.; Eskridge, K.M.; Isom, L.D.; Hanna, M.A. Extraction, identification, and quantification of antioxidant phenolics from hazelnut (*Corylus avellana* L.) shells. *Food Chem.* **2018**, *244*, 7–15. [CrossRef]
25. Yuan, B.; Lu, M.; Eskridge, K.M.; Hanna, M.A. Valorization of hazelnut shells into natural antioxidants by ultrasound-assisted extraction: Process optimization and phenolic composition identification. *J. Food Process Eng.* **2018**, *41*, 1–13. [CrossRef]
26. Esposito, T.; Sansone, F.; Franceschelli, S.; Del Gaudio, P.; Picerno, P.; Aquino, R.P.; Mencherini, T. Hazelnut (*Corylus avellana* L.) shells extract: Phenolic composition, antioxidant effect and cytotoxic activity on human cancer cell lines. *Int. J. Mol. Sci.* **2017**, *18*, 392. [CrossRef] [PubMed]
27. Surek, E.; Buyukkileci, A.O. Production of xylooligosaccharides by autohydrolysis of hazelnut (*Corylus avellana* L.) shell. *Carbohydr. Polym.* **2017**, *174*, 565–571. [CrossRef]
28. Midilli, A.; Rzayev, P.; Olgun, H.; Ayhan, T. Solar hydrogen production from hazelnut shells. *Int. J. Hydrogen Energy* **2000**, *25*, 723–732. [CrossRef]

29. Midilli, A.; Dogru, M.; Howarth, C.R.; Ayhan, T. Hydrogen production from hazelnut shell by applying air-blown downdraft gasification technique. *Int. J. Hydrogen Energy* **2001**, *26*, 29–37. [CrossRef]

30. Hoşgün, E.Z.; Berikten, D.; Kıvanç, M.; Bozan, B. Ethanol production from hazelnut shells through enzymatic saccharification and fermentation by low-temperature alkali pretreatment. *Fuel* **2017**, *196*, 280–287. [CrossRef]

31. Fuso, A.; Risso, D.; Rosso, G.; Rosso, F.; Manini, F.; Manera, I.; Caligiani, A. Potential valorization of hazelnut shells through extraction, purification and structural characterization of prebiotic compounds: A critical review. *Foods* **2021**, *10*, 1197. [CrossRef]

32. Badalyan, S.; Zambonelli, A. The potential of mushrooms to develop healthy food and biotech products. In *Fungi and Fungal Products in Human Welfare and Biotechnology*; Satyanarayana, T., Deshmukh, S.K., Eds.; Springer Nature: Berlin/Heidelberg, Germany, 2022.

33. Royse, D.J.; Baars, J.; Tan, Q. Current overview of mushroom production in the world. In *Edible and Medicinal Mushrooms: Technology and Applications*; Zied, D.C., Pardo-Giménez, A., Eds.; John Wiley & Sons Ltd.: Chichester, UK, 2017; pp. 5–13.

34. Vedder, J.C.; Van den Munckhof-Vedder, M. *Modern Mushroom Growing 2020 Harvesting*; Vedder, P.J.C., Ed.; Harvest House: Irvine, CA, USA, 2020.

35. Wang, L.; Li, J.Q.; Zhang, J.; Li, Z.M.; Liu, H.G.; Wang, Y.Z. Traditional uses, chemical components and pharmacological activities of the genus: *Ganoderma* P. Karst.: A review. *RSC Adv.* **2020**, *10*, 42084–42097. [CrossRef]

36. Di Piazza, S.; Benvenuti, M.; Damonte, G.; Cecchi, G.; Mariotti, M.G.; Zotti, M. Fungi and circular economy: *Pleurotus ostreatus* grown on a substrate with agricultural waste of lavender, and its promising biochemical profile. *Recycling* **2021**, *6*, 40. [CrossRef]

37. Pekşen, A.; Küçükomuzlu, B. Yield potential and quality of some *Pleurotus* species grown in substrates containing hazelnut husk. *Pak. J. Biol. Sci.* **2004**, *7*, 768–771. [CrossRef]

38. Yildiz, S.; Yildiz, Ü.C.; Gezer, E.D.; Temiz, A. Some lignocellulosic wastes used as raw material in cultivation of the *Pleurotus ostreatus* culture mushroom. *Process Biochem.* **2002**, *38*, 301–306. [CrossRef]

39. Coates, J. Interpretation of infrared spectra, a practical approach. In *Encyclopedia of Analytical Chemistry*; Meyers, R.A., Ed.; John Wiley & Sons Ltd.: Chichester, UK, 2006; pp. 10815–10837.

40. Li, X.P.; Li, J.; Liu, H.; Wang, Y.Z. A new analytical method for discrimination of species in *Ganodermataceae* mushrooms. *Int. J. Food Prop.* **2020**, *23*, 227–240. [CrossRef]

41. Pin, M.W.; Park, E.J.; Choi, S.; Kim, Y.I.; Jeon, C.H.; Ha, T.H.; Kim, Y.H. Atomistic evolution during the phase transition on a metastable single NaYF4:Yb,Er upconversion nanoparticle. *Sci. Rep.* **2018**, *8*, 1–10. [CrossRef]

42. Bekiaris, G.; Tagkouli, D.; Koutrotsios, G.; Kalogeropoulos, N.; Zervakis, G.I. *Pleurotus* mushrooms content in glucans and ergosterol assessed by ATR-FTIR spectroscopy and multivariate analysis. *Foods* **2020**, *9*, 535. [CrossRef]

43. O'Gorman, A.; Downey, G.; Gowen, A.A.; Barry-Ryan, C.; Frias, J.M. Use of fourier transform infrared spectroscopy and chemometric data analysis to evaluate damage and age in mushrooms (*Agaricus bisporus*) grown in Ireland. *J. Agric. Food Chem.* **2010**, *58*, 7770–7776. [CrossRef]

44. Fornito, S.; Puliga, F.; Leonardi, P.; Di Foggia, M.; Zambonelli, A.; Francioso, O. Degradative ability of mushrooms cultivated on corn silage digestate. *Molecules* **2020**, *25*, 3020. [CrossRef]

45. Bekiaris, G.; Koutrotsios, G.; Tarantilis, P.A.; Pappas, C.S.; Zervakis, G.I. FTIR assessment of compositional changes in ligno-cellulosic wastes during cultivation of *Cyclocybe cylindracea* mushrooms and use of chemometric models to predict production performance. *J. Mater. Cycles Waste Manag.* **2020**, *22*, 1027–1035. [CrossRef]

46. Tryfinopoulou, P.; Chourdaki, A.; Nychas, G.J.E.; Panagou, E.Z. Competitive yeast action against *Aspergillus carbonarius* growth and ochratoxin A production. *Int. J. Food Microbiol.* **2020**, *317*, 108460. [CrossRef]

47. Sinclair, C.G.; Cantero, D. Fermentation modelling. In *Fermentation a Practical Approach*; McNeil, B.L., Harvey, M., Eds.; IRL Press: New York, NY, USA, 1989; pp. 65–112.

48. Oei, P. *Mushroom Cultivation IV: Appropriate Technology for Mushroom Growers*; ECO Consult Foundation: Amsterdam, The Netherlands, 2016.

49. Zhang, H.; Peng, J.; Zhang, Y.R.; Liu, Q.; Pan, L.Q.; Tu, K. Discrimination of volatiles of shiitakes (*Lentinula edodes*) produced during drying process by electronic nose. *Int. J. Food Eng.* **2020**, *16*, 1–13. [CrossRef]

50. Chang, S.T.; Lau, O.W.; Cho, K.Y. The cultivation and nutritional value of *Pleurotus sajor-caju*. *Eur. J. Appl. Microbiol. Biotechnol.* **1981**, *12*, 58–62. [CrossRef]

51. R Studio. Available online: https://www.rstudio.com (accessed on 6 February 2022).

52. Rahman, M.R.; Hamdan, S.; Lai, J.C.H.; Jawaid, M.; Yusof, F.A.; Bin, M. Physico-mechanical, thermal and morphological properties of furfuryl alcohol/2-ethylhexyl methacrylate/halloysite nanoclay wood polymer nanocomposites (WPNCs). *Heliyon* **2017**, *3*, e00342. [CrossRef] [PubMed]

53. Mohebby, B. Attenuated total reflection infrared spectroscopy of white-rot decayed beech wood. *Int. Biodeterior. Biodegrad.* **2005**, *55*, 247–251. [CrossRef]

54. Popescu, C.M.; Popescu, M.C.; Vasile, C. Structural changes in biodegraded lime wood. *Carbohydr. Polym.* **2010**, *79*, 362–372. [CrossRef]

55. Singh, S.; Harms, H.; Schlosser, D. Screening of ecologically diverse fungi for their potential to pretreat lignocellulosic bioenergy feedstock. *Appl. Microbiol. Biotechnol.* **2014**, *98*, 3355–3370. [CrossRef]

56. Huang, X.; Kocaefe, D.; Kocaefe, Y.; Boluk, Y.; Pichette, A. Study of the degradation behavior of heat-treated jack pine (*Pinus banksiana*) under artificial sunlight irradiation. *Polym. Degrad. Stab.* **2012**, *97*, 1197–1214. [CrossRef]

57. Bekiaris, G.; Lindedam, J.; Peltre, C.; Decker, S.R.; Turner, G.B.; Magid, J.; Bruun, S. Rapid estimation of sugar release from winter wheat straw during bioethanol production using FTIR-photoacoustic spectroscopy. *Biotechnol. Biofuels* **2015**, *8*, 1–12. [CrossRef]

58. Fan, M.; Dai, D.; Huang, B. Fourier transform infrared spectroscopy for natural fibres. *Fourier Transform-Mater. Anal.* **2012**, *3*, 45–68.

59. De Rosa, I.M.; Kenny, J.M.; Puglia, D.; Santulli, C.; Sarasini, F. Morphological, thermal and mechanical characterization of okra (*Abelmoschus esculentus*) fibres as potential reinforcement in polymer composites. *Compos. Sci. Technol.* **2010**, *70*, 116–122. [CrossRef]

60. Pandey, K.K.; Pitman, A.J. FTIR studies of the changes in wood chemistry following decay by brown-rot and white-rot fungi. *Int. Biodeterior. Biodegrad.* **2003**, *52*, 151–160. [CrossRef]

61. Zervakis, G.I.; Bekiaris, G.; Tarantilis, P.A.; Pappas, C.S. Rapid strain classification and taxa delimitation within the edible mushroom genus *Pleurotus* through the use of diffuse reflectance infrared Fourier transform (DRIFT) spectroscopy. *Fungal Biol.* **2012**, *116*, 715–728. [CrossRef] [PubMed]

62. Choong, Y.K.; Sun, S.Q.; Zhou, Q.; Ismail, Z.; Rashid, B.A.A.; Tao, J.X. Determination of storage stability of the crude extracts of *Ganoderma lucidum* using FTIR and 2D-IR spectroscopy. *Vib. Spectrosc.* **2011**, *57*, 87–96. [CrossRef]

63. Mohaček-Grošev, V.; Božac, R.; Puppels, G.J. Vibrational spectroscopic characterization of wild growing mushrooms and toadstools. *Spectrochim. Acta Part A Mol. Biomol. Spectrosc.* **2001**, *57*, 2815–2829. [CrossRef]

64. Das, B.; Rajkonwar, J.; Jagannath, A.; Raul, P.K.; Deb, U. Infra-red spectra of different species of cultivated oyster mushrooms: Possible tool for identifying bioactive compounds and establishing taxonomic linkage. *Def. Life Sci. J.* **2020**, *5*, 118–124. [CrossRef]

65. Melanouri, E.M.; Dedousi, M.; Diamantopoulou, P. Cultivating *Pleurotus ostreatus* and *Pleurotus eryngii* mushroom strains on agro-industrial residues in solid-state fermentation. Part II: Effect on productivity and quality of carposomes. *Carbon Resour. Convers.* **2022**, *5*, 52–60. [CrossRef]

66. Şenol, H. Biogas potential of hazelnut shells and hazelnut wastes in Giresun City. *Biotechnol. Rep.* **2019**, *24*, e00361. [CrossRef]

67. Kaya, N.; Yıldız, Z.; Ceylan, S. Preparation and characterisation of biochar from hazelnut shell and its adsorption properties for methylene blue dye. *J. Polytech.* **2018**, *21*, 765–776. [CrossRef]

68. Kumla, J.; Suwannarach, N.; Sujarit, K.; Penkhrue, W.; Kakumyan, P.; Jatuwong, K.; Vadthanarat, S.; Lumyong, S. Cultivation of mushrooms and their lignocellulolytic enzyme production through the utilization of agro-industrial waste. *Molecules* **2020**, *25*, 2811. [CrossRef]

69. Stamets, P. *Growing Gourmet and Medicinal Mushrooms*; Ten Speed Press: Berkeley, CA, USA, 2000.

70. Tamaki, Y.; Mazza, G. Rapid determination of lignin content of straw using Fourier transform mid-infrared spectroscopy. *J. Agric. Food Chem.* **2011**, *59*, 504–512. [CrossRef] [PubMed]

71. Del Río, J.C.; Rencoret, J.; Prinsen, P.; Martínez, Á.T.; Gutiérrez, A.; Ralph, J. Structural characterization of wheat straw lignin. Evidence for a novel monomer in grasses. *Cons. Super. Investig. Científicas* **2013**. Available online: https://digital.csic.es/bitstream/10261/86427/1/JCdelRio-17ISWFPC-proceeding.pdf. (accessed on 16 December 2021).

72. Pettersen, R.C. The chemical composition of wood. In *The Chemistry of Solid Wood*; American Chemical Society: New York, NY, USA, 1984; pp. 57–126.

73. Le Floch, A.; Jourdes, M.; Teissedre, P.L. Polysaccharides and lignin from oak wood used in cooperage: Composition, interest, assays: A review. *Carbohydr. Res.* **2015**, *417*, 94–102. [CrossRef] [PubMed]

74. Vinciguerra, V.; Spina, S.; Luna, M.; Petrucci, G.; Romagnoli, M. Structural analysis of lignin in chestnut wood by pyrolysis-gas chromatography/mass spectrometry. *J. Anal. Appl. Pyrolysis* **2011**, *92*, 273–279. [CrossRef]

75. Madeira, J.V.; Contesini, F.J.; Calzado, F.; Rubio, M.V.; Zubieta, M.P.; Lopes, D.B.; de Melo, R.R. Agro-industrial residues and microbial enzymes: An Overview on the eco-friendly bioconversion into high value-added products. In *Biotechnology of Microbial Enzymes: Production, Biocatalysis and Industrial Applications*; Elsevier, Inc.: London, UK, 2017; pp. 475–511; ISBN 9780128037461.

76. Jurak, E.; Patyshakuliyeva, A.; De Vries, R.P.; Gruppen, H.; Kabel, M.A. Compost grown *Agaricus bisporus* lacks the ability to degrade and consume highly substituted xylan fragments. *PLoS ONE* **2015**, *10*, e0134169. [CrossRef]

77. Nandni, S.; Mishra, S. Crop room studies in relation to yield potential of *Lentinula edodes* strains on wheat straw. *J. Hill Agric.* **2018**, *9*, 124. [CrossRef]

78. Kalmiş, E.; Sargin, S. Cultivation of two *Pleurotus* species on wheat straw substrates containing olive mill waste water. *Int. Biodeterior. Biodegrad.* **2004**, *53*, 43–47. [CrossRef]

79. Ćilerdžić, J.L.; Vukojević, J.B.; Klaus, A.S.; Ivanović, Ž.S.; Blagojević, J.D.; Stajić, M.M. Wheat straw—A promising substrate for *Ganoderma lucidum* cultivation. *Acta Sci. Pol. Hortorum Cultus* **2018**, *17*, 13–22. [CrossRef]

80. Ritz, K.; Crawford, J.W. Colony development in nutritionally heterogeneous environments. In *The Fungal Colony*; Gow, N.A.R., Robson, G.D., Gadd, G.M., Eds.; Cambridge University Press: Cambridge, UK, 1999; pp. 49–74.

81. Bruhn, J.; Hall, M. Growing Shiitake Mushrooms in an Agroforestry Practice. Available online: https://centerforagroforestry.org/wp-content/uploads/2021/05/af1010 (accessed on 16 December 2021).

82. Zivanovic, S.; Busher, R.W.; Kim, K.S. Textural changes in mushrooms (*Agaricus bisporus*) associated with tissue ultrastructure and composition. *J. Food Sci.* **2000**, *65*, 1404–1408. [CrossRef]